SOME EFFECTS OF SHIMS AND WASHERS ON THE ACOL QUADRUPOLES

M R Harold

15/3/85

Introduction

All ACOL quadrupoles will be fitted with detachable end shims. It is the intention to machine these shims so as to make relatively coarse adjustments to the effective length and field shape. Fine adjustments of the length will be achieved by the use of thin shims, and the field shape will be tuned by means of washers. In order to estimate the effectiveness of some of these adjustments, TOSCA has been used in three ways ie:

1) for an oversize shim on the QN.

2) for an angled shim on the QWS (QFW8) to change the sextupole component.

3) for simulated washer packs in a few positions on the QWS (QFW8).

In order to produce results more quickly, both types of quadrupole have been modelled with coarser meshes than those which were used to determine their profile [(1)].

QN with end shims

Fig 1 shows the mesh used, with the pole-shim area in black. Fig 2 is an oblique side-view of the magnet, showing a shim of excess length 15 mm. The core length was 600 mm, and computations were done for ampere terms of 1883 x 17 (QN4) and 1883 x 15 (QN5) with and without the excess 15 mm at each pole end.

The gradient integrals are shown in Fig 3; the agreement with the original QN work is not good, but they do suggest that some washer-shimming may be necessary for $x > 100$ mm.

A summary of the results is given in Table 1. Note that these have been corrected for a core length of 607 mm rather than 600 mm, and that in calculating the effective length (L_{eff}) of (QN + Shims) the g_0 of (QN - Shims) has been used as the devisor.

The results show that

a) the central gradient falls by $\sim 1\,\%$ when the shims are added.

b) for QN4 the shims are $\sim 60\,\%$ efficient in increasing L_{eff}

c) for QN5 the shims are $\sim 72\,\%$ efficient in increasing L_{eff}

TABLE 1

	QN4 - Shims	QN4 + Shims	QN5 - Shims	QN5 + Shims
g_0 (T/m)	6.285	6.223	5.6985	5.658
$\int gdz$ (T)	4.49883	4.61194	4.08578	4.20877
L_{eff} (m)	0.7158	0.7338	0.7170	0.7836
ΔL_{eff} (m)		0.0180		0.0216

QW with angled shims

First-order changes to the sextupole components in the QW's can be effected by machining the shim-end faces so that they are no longer at right-angles to the axis of the quadupole. The change in sextupole strength can be easily calculated, but it was required to know whether the high degree of saturation in parts of the QFW8 poles could have a significant effect.

The mesh is shown in Fig 4, with the shim areas cross-hatched. The way in which the shims were angled is illustrated in Fig 5 - one shim projects beyond the pole-end, and the other is recessed. Fig 6 gives the TOSCA results for the case QWSHOE, where there is no angle on the shims (cf Fig 8 in ref. 1), and Fig 7 shows the difference between QWSTIL (angled shims) and QWSHOE.

If we neglect end effects, the gradient integral as a function of horizontal displacement can be expresed as

$$G(x) = gL + B'' xL + 2ax(g + B'' x)$$

Where L = total iron length
g = central quadrupole component
B'' = built-in sextupole component
x = horizontal displacement
a = angle of cut on the shims ($\tan a \approx a$)

Then $$\frac{\Delta G}{G} = \frac{B'' xL + 2ax(g + B''x)}{gL}$$

and $$\frac{\Delta G}{G} - \frac{K' x}{K} = \frac{2ax}{L}\left(1 + \frac{K' x}{K}\right),$$ where K and K' have their usual meanings.

For QFW8, L = 0.62 m, K'/K = 0.7477, and we used a = 0.01859 rad.

The difference between a = 0.01859 and a = 0 is then

$$0.06x + 0.04486x^2, \text{ x in metres.}$$

This is also plotted on Fig 7. The agreement with the analysis is quite good, and one concludes that the sextupole component can be modified in this way by about 10% without higher harmonics of large amplitude being introduced.

QW with washers

In order to simulate the effects of washer packs attached to the QWS pole-ends, the mesh was re-structured (see Fig 8 for details of region of interest) so that any iron region could be extended azimuthally by 1 or 2 cm. Only 90° of the magnet was described (the C profile, which involves the highest fields) in order to decrease the job turn-round time. Consequently the field gradient integral was no longer linear (see Fig 9) but the fields in the region of the washer packs were typical of the full quadrupole.

The programme was run for the following conditions:

Region	Depth (cm)						
A + B	0	1	2	0	0	0	0
C	0	0	0	1	2	0	0
D	0	0	0	0	0	1	2

The gradient results for (0, 0, 0) were subtracted from all the others, and these are plotted in Fig 10. It is apparent that some saturation is taking place, in that 2 cm is not twice as effective as 1 cm, but it is likely that some useful effect could still be achieved beyond 2 cm.

Finally, if one predicts from these answers what the combination (2, 1, 1) would result in, one gets the solid line in Fig 11. Here the abcissa is plotted on an x^4 scale, and the linear rise as far as 13 cm represents a 12-pole correction. The TOSCA results are shown to agree with the prediction to within 0.1% up to a radius of 17 cm, but we should not put too much reliance on these figures. We can conclude , however, that local gradient-integral perturbations of the order of 1% can be achieved with washer packs in the high-field region of the QWS.

Reference

1. The pole profile design of the ACOL quadrupoles
   M R Harold and H H Umstatter. PS/AA/ACOL Note 31

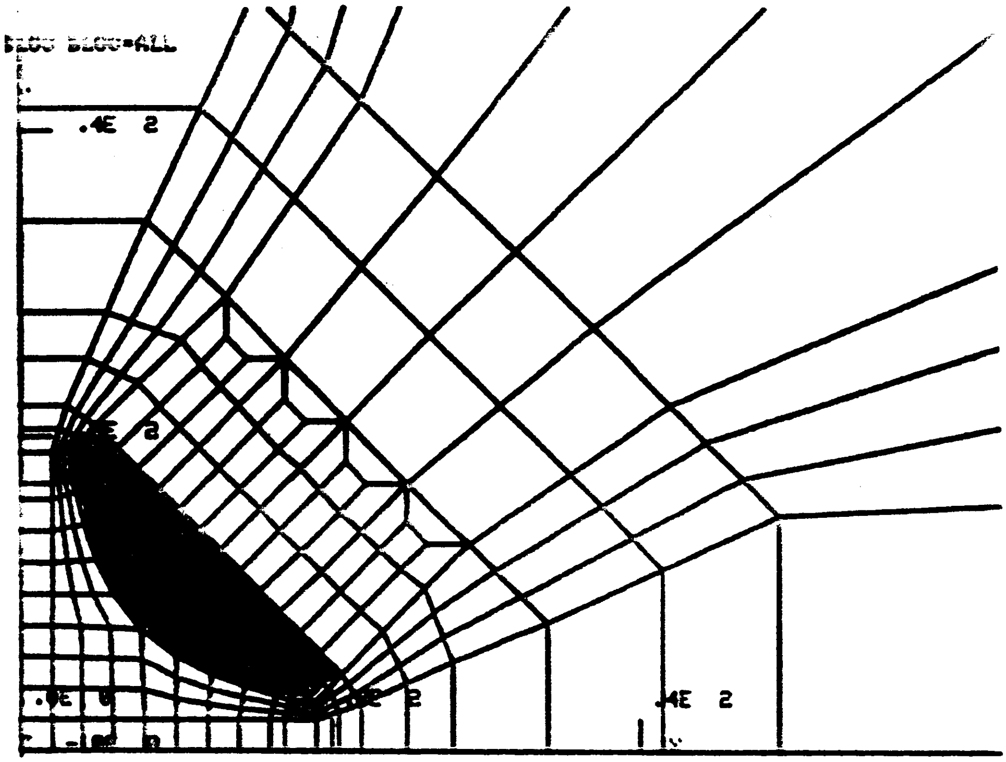

Fig 1

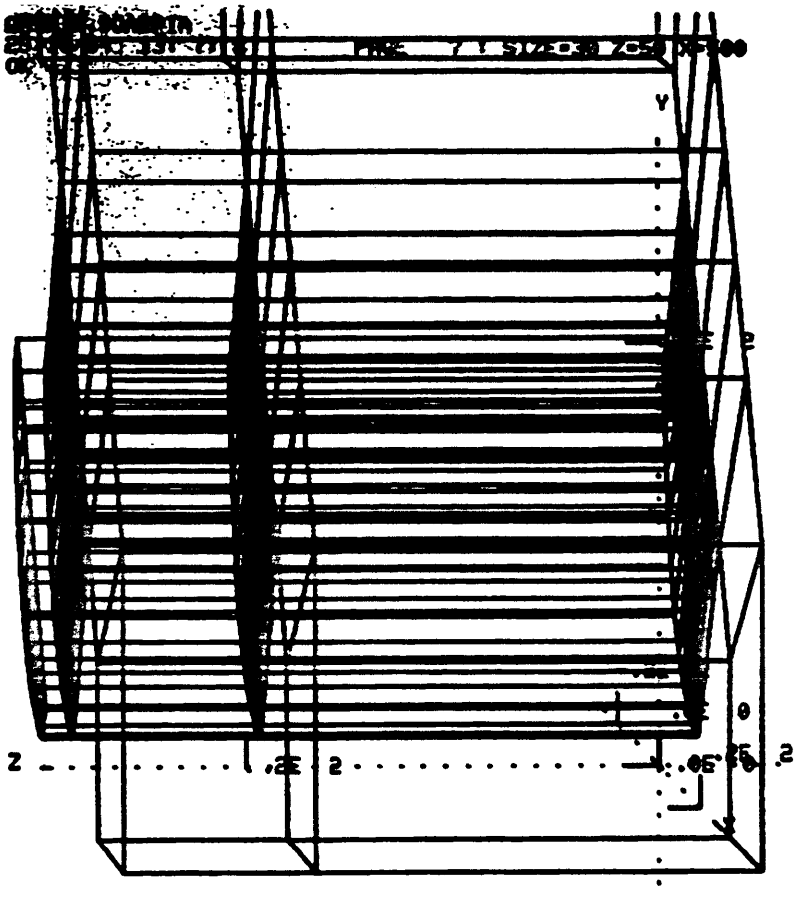

Fig 2

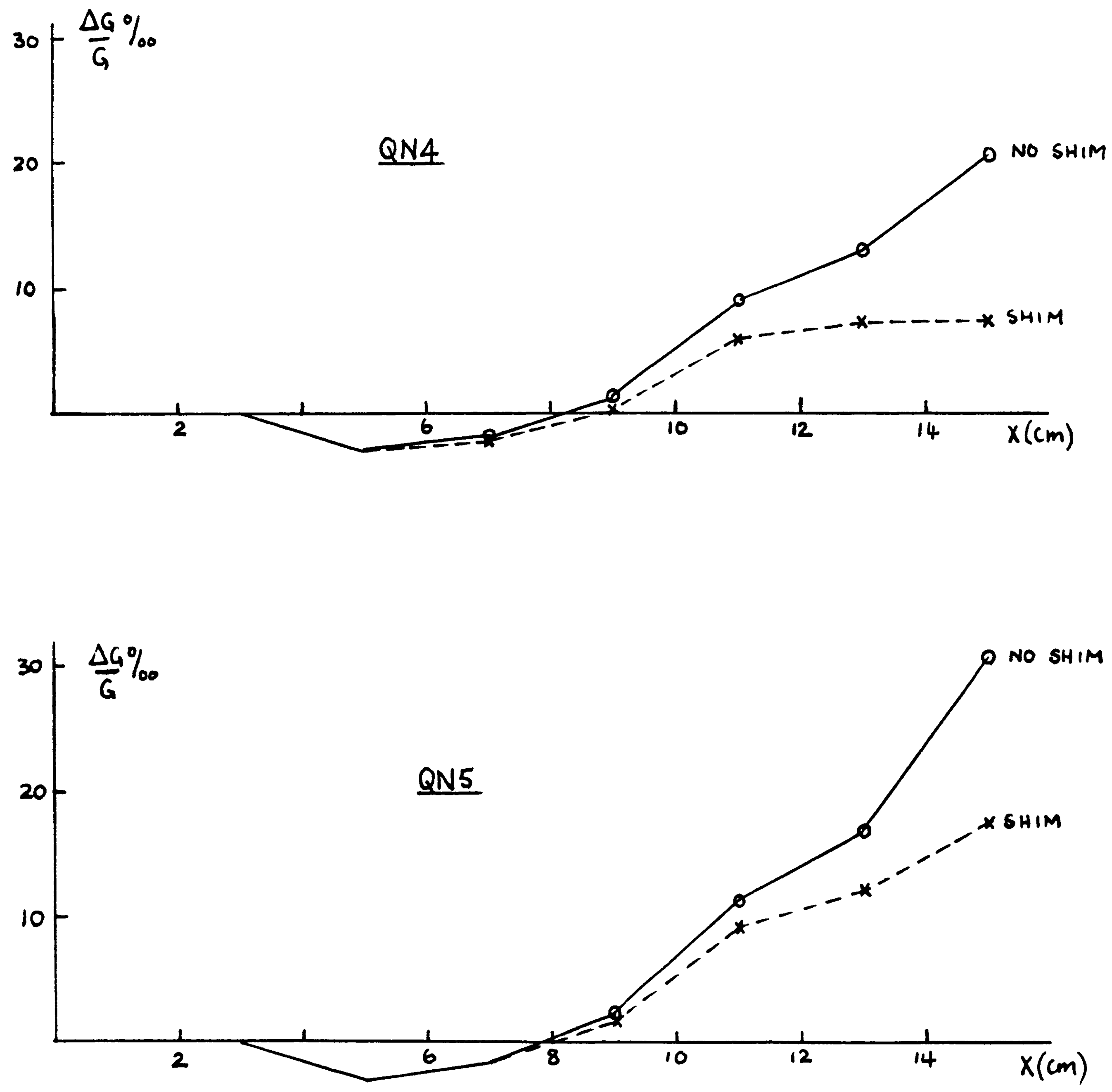
ΔG/G ‰
30
20
10
QN4
NO SHIM
SHIM
2
6
10
12
14
X(cm)
ΔG/G ‰
30
20
10
QN5
NO SHIM
SHIM
2
6
8
10
12
14
X(cm)

Fig 3

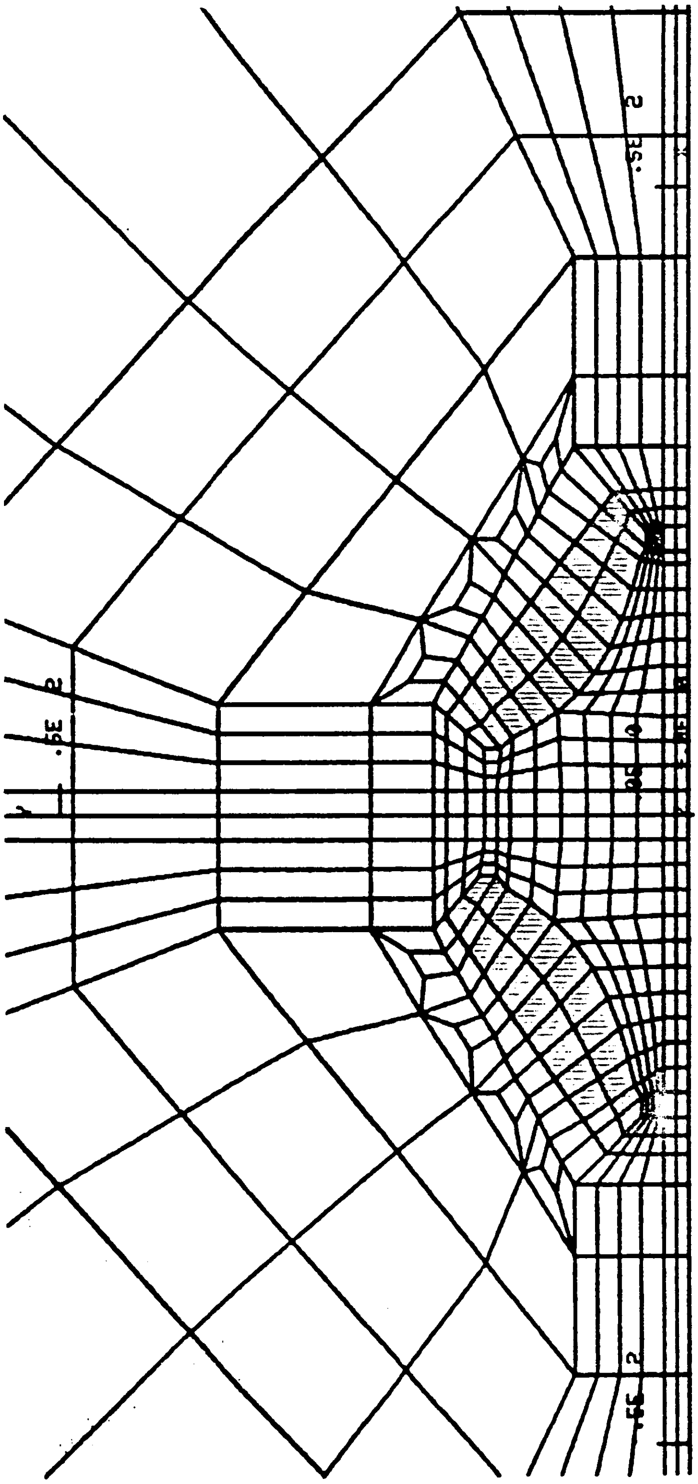

Fig 4

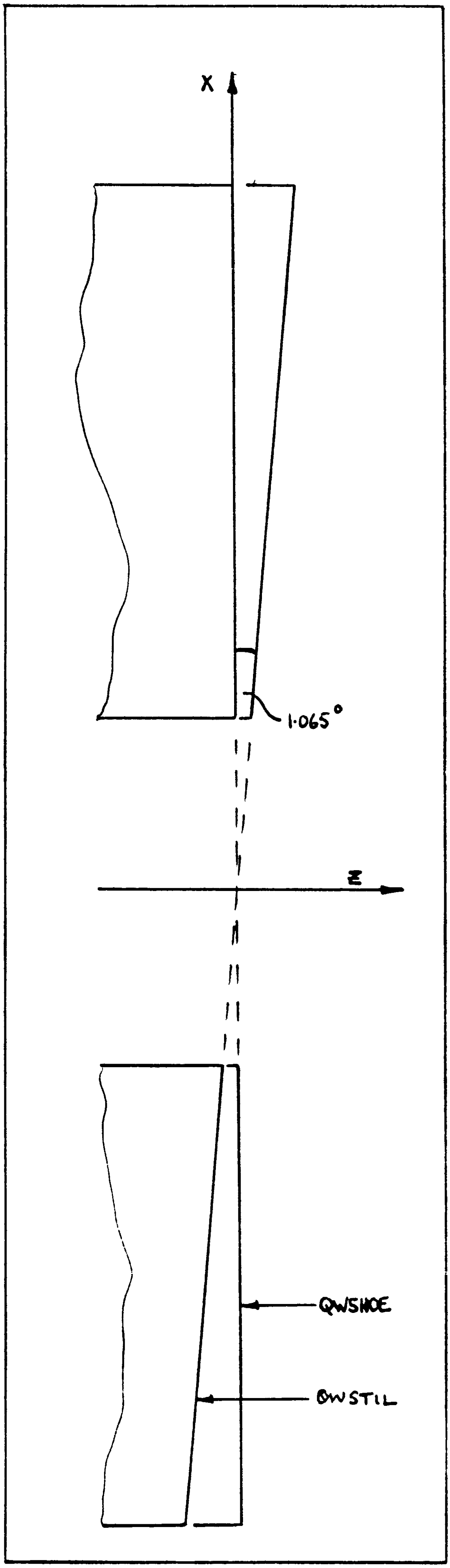

Fig 5

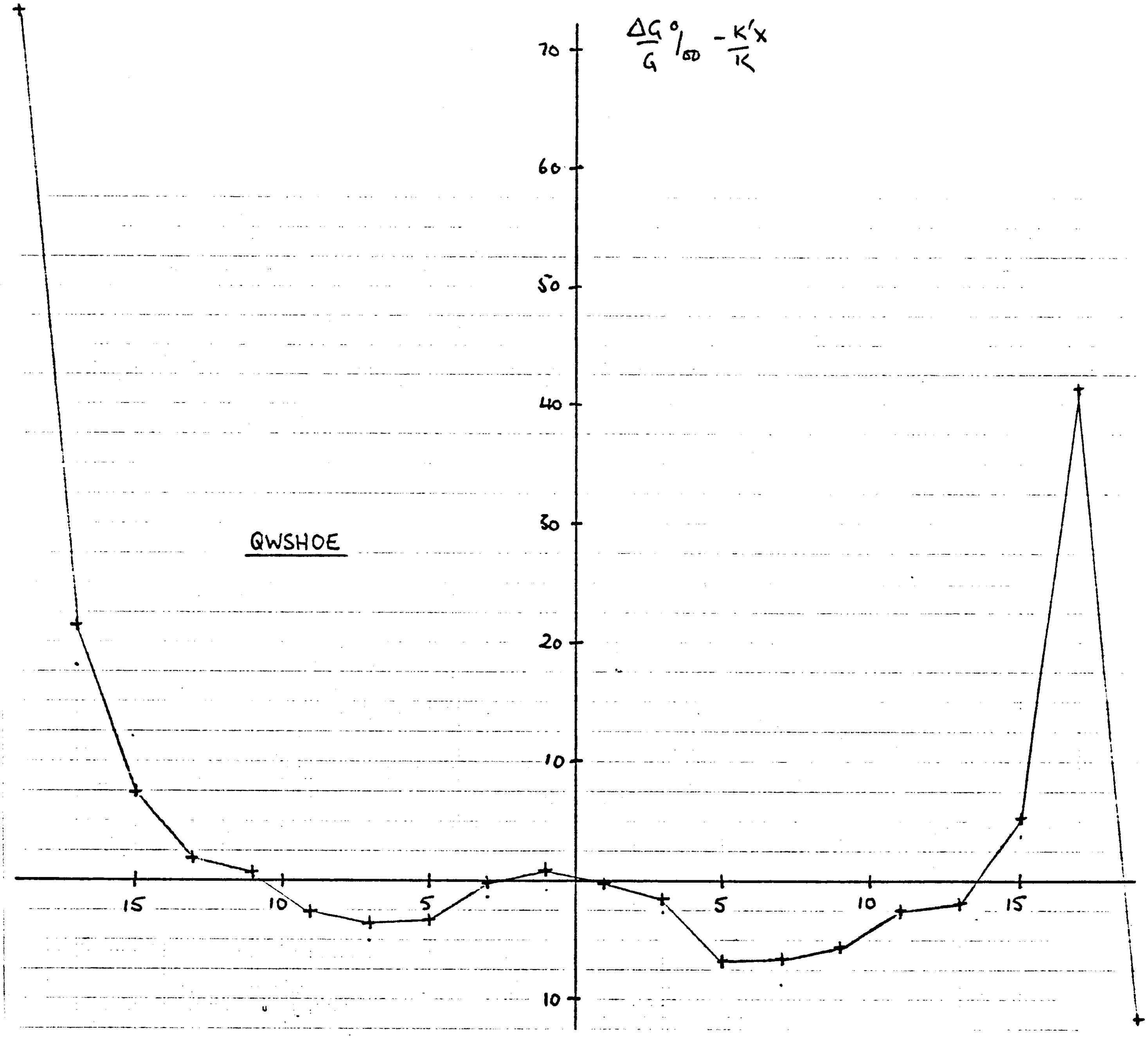

ΔG/G ‰ − K'x/K
70
60
50
40
30
20
10
10
QWSHOE
15
10
5
5
10
15

Fig 6

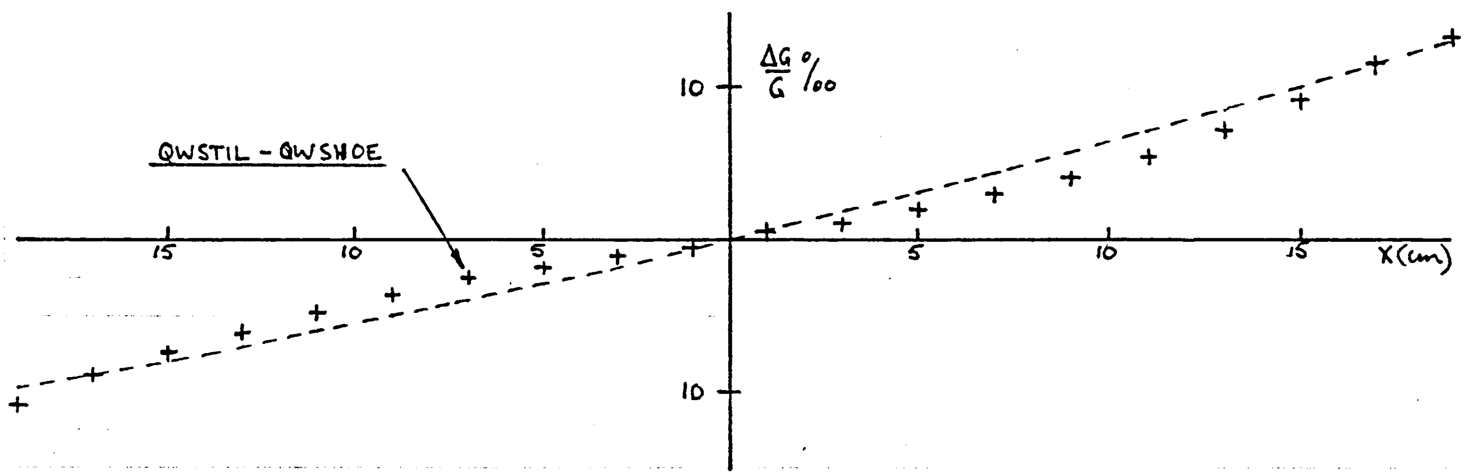

ΔG/G ‰
10
10
QWSTIL - QWSHOE
15
10
5
5
10
15
X(cm)

Fig 7

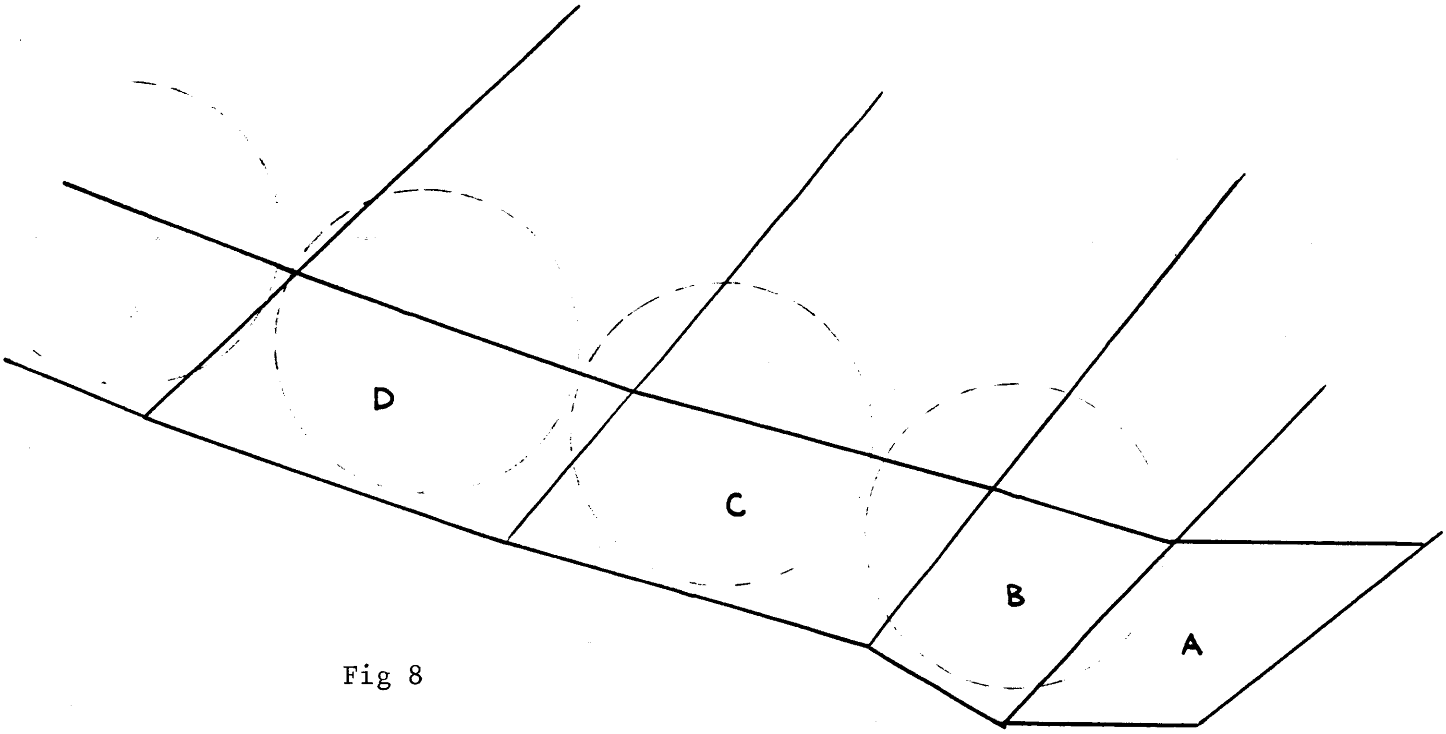

Fig 8

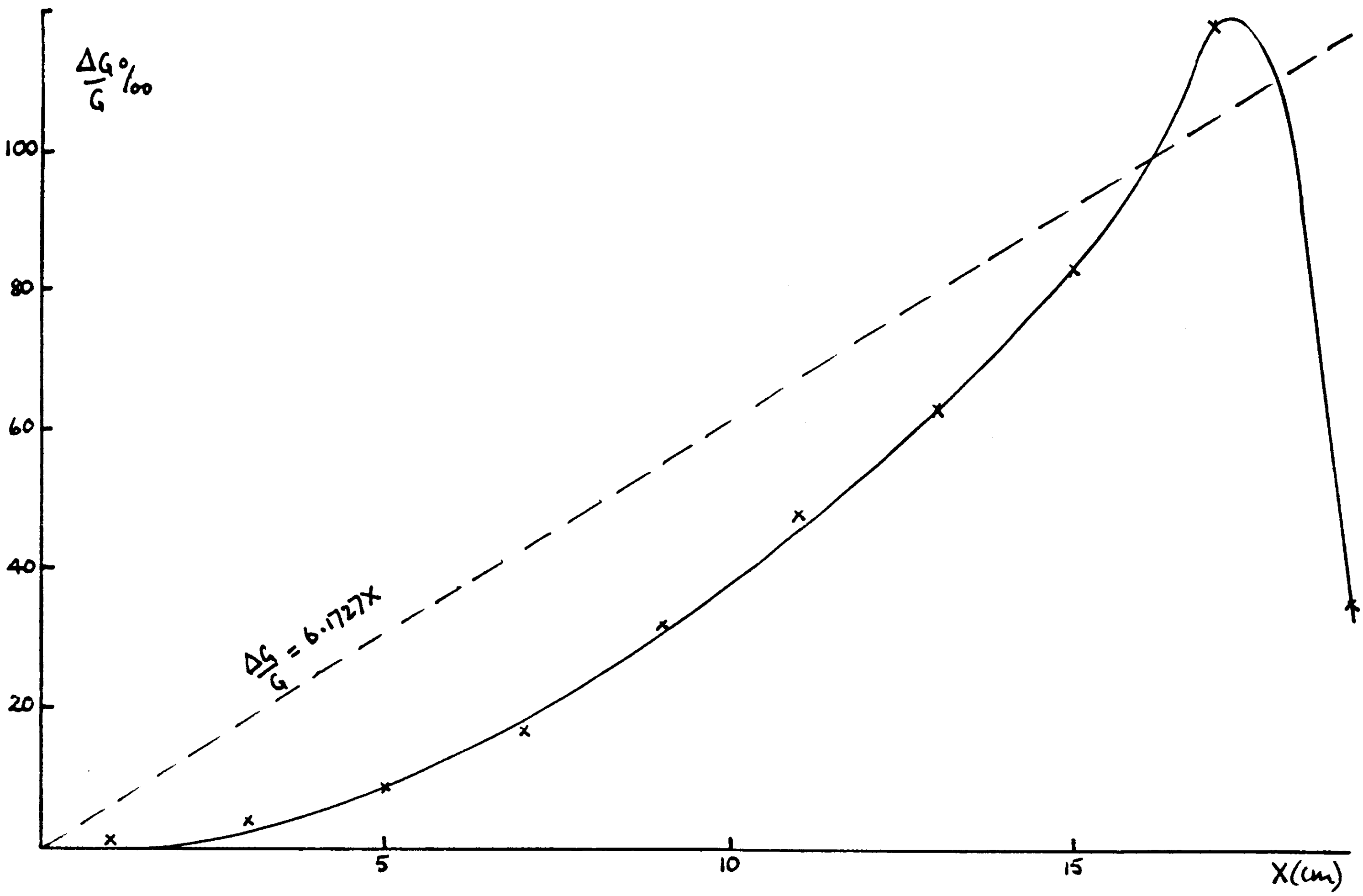

Fig 9

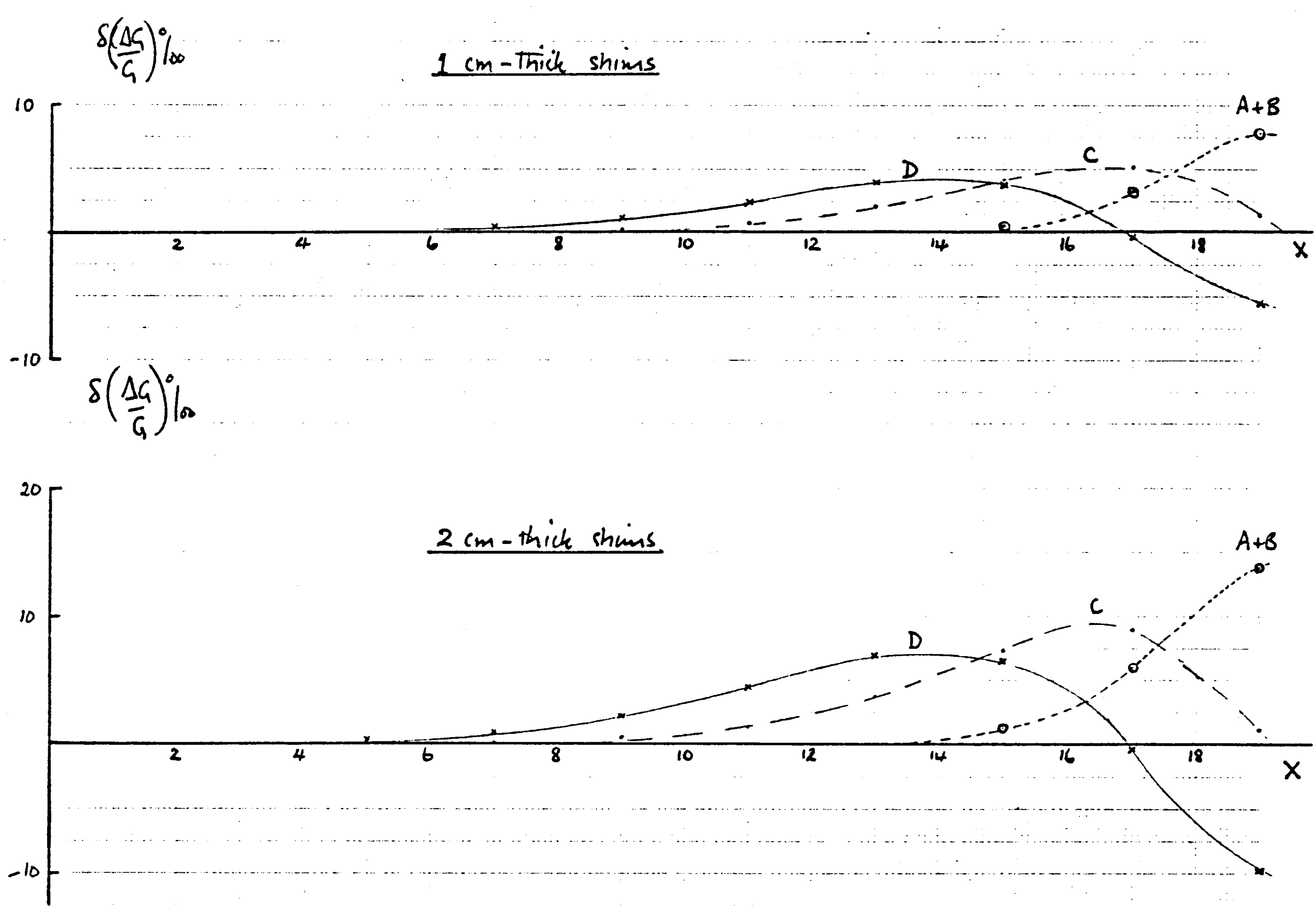

δ(ΔG/G)°/oo
1 cm-Thick shims
10
-10
A+B
C
D
2
4
6
8
10
12
14
16
18
X
δ(ΔG/G)°/oo
20
2 cm-thick shims
10
-10
A+B
C
D
2
4
6
8
10
12
14
16
18
X

Fig 10

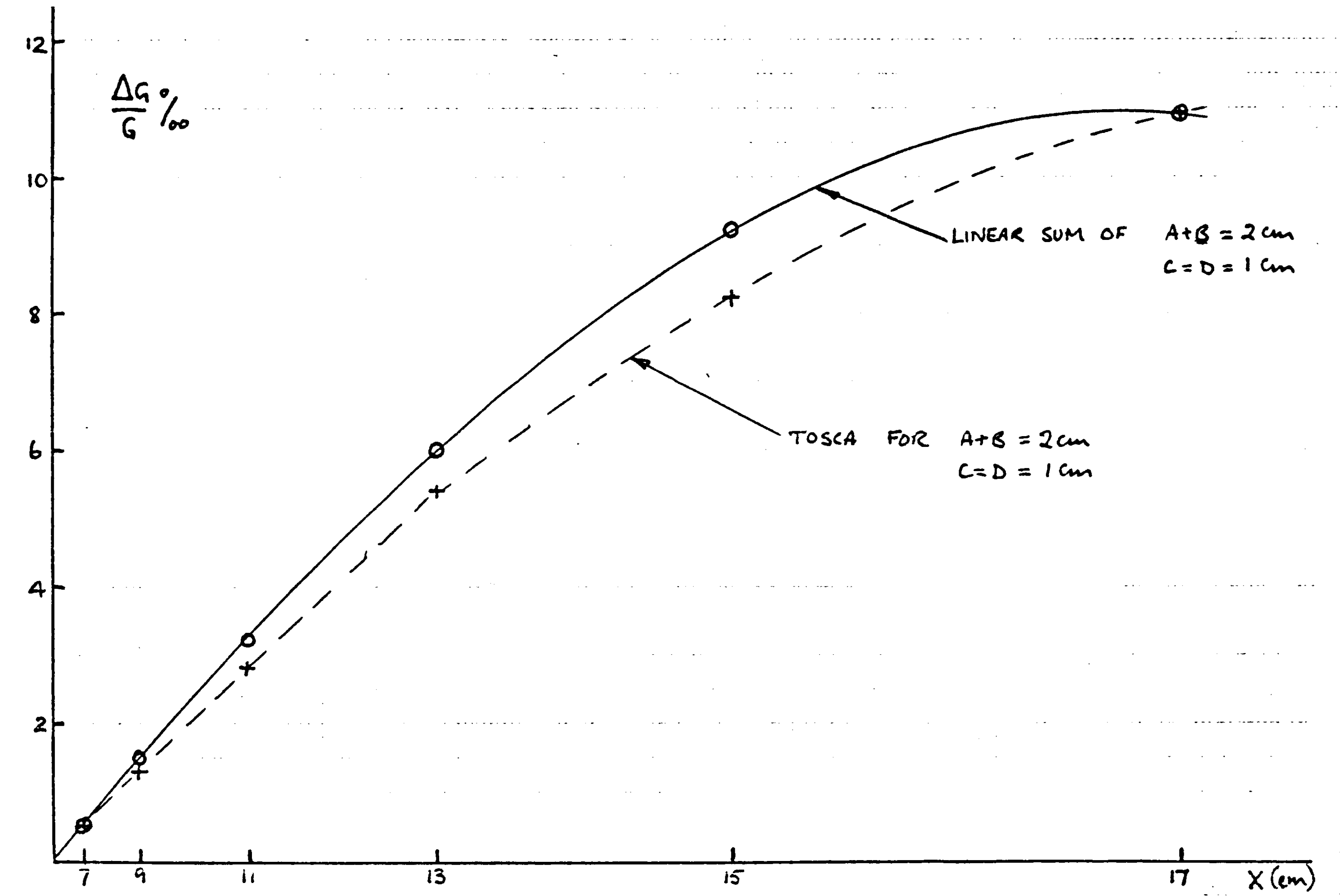

ΔG/G °/oo
12
10
8
6
4
2
LINEAR SUM OF A+B = 2 cm
C = D = 1 cm
TOSCA FOR A+B = 2 cm
C = D = 1 cm
7
9
11
13
15
17
X (cm)

Fig 11